



## Composite Beams of Cold Formed Steel Section and Concrete Slab

<sup>1</sup>S.A.Hassaneen, <sup>2</sup>M.R.Badr, <sup>3</sup>E.S.Salem and <sup>4</sup>M.A.Youns

<sup>1</sup> Professor, Civil Engineering Department, Al Azhar University, Egypt.

<sup>2</sup> Professor, Civil Engineering Department, The researches Center for Housing and Building, Egypt.

<sup>3</sup> Associate professor, Civil Engineering Department, Al Azhar University, Egypt.

<sup>4</sup> Assistant lecturer, Civil Engineering Department, Al Azhar University, Egypt.

### ملخص البحث

انتشرت بشكل واسع في المباني استخدام الكمرات المركبة من قطاع معدني وبلاطة خرسانية سواء كان القطاع المعدني مشكل على الساخن او البارد. استخدمنا في هذا البحث كمرات مركبة من قطاع معدني مشكل على البارد وبلاطة خرسانية. تم اقتراح رابط قص يكون سهل التشكيل يربط القطاع المعدني والبلاطة الخرسانية. تم عمل اختبارات عملية على كمرات مركبة تختلف في نوع رابط القص المقترح وسمك القطاع المعدني المشكل على البارد وكذلك سمك البلاطة الخرسانية وذلك لدراسة سلوك هذا النوع من الكمرات المركبة. قد بينت النتائج زيادة في الحمل الاقصى للكمرات المركبة نتيجة لروابط القص المقترحة وكذلك نتيجة لزيادة سمك القطاع المعدني او زيادة سمك البلاطة الخرسانية.

### Abstract

This work presents experimental tests which were carried out to examine the structural behavior of composite beams of cold formed steel sections with concrete slab. Seven innovative composite beams cold formed steel lipped channel sections (CFS) with concrete slab, taken into account the effect of bent up half flange for the channel as a new shear dowels, were studied. The test parameters include the shape of shear dowels, the thickness of CFS and the concrete slab thickness. The results showed that by increasing the thickness of CFS leads to an increase in the ultimate load of the composite beams. Furthermore, by increasing the thickness of the concrete slab will provide an increase in the ultimate load.

**Keywords:** Composite; Cold-formed; Large-scale test; Bent-up half flange channel; Flexural capacity; shear dowels.

### 1. Introduction

In recent years, composite construction becomes more popular and broadly accounts for the dominance of steel frames in the construction sector in many developing countries. The main structural benefits of using composite beams can be listed as follows:

1. Savings in steel weight are typically 30 to 50% over non-composite beams relied on hot-rolled sections due to greater stiffness.
2. The main economy sought in buildings is speed of construction.

Cold-formed steel (CFS) sections, usually between 1.2 mm to 3.2 mm thickness, have been recognized as an important contributor to sustainable structures in the developed nations. Recent studies on composite beams with CFS had been reported by other researchers who agree about the application of CFS beams and composites with concrete [1]. However, there remains a lack of data on the behavior and performance of CFS in composite construction. One limiting advantage of CFS is the thinness of its section that makes it susceptible to torsional, distortional; lateral torsional, lateral distortional and local buckling. Hence, a sensible solution is resorting to a composite construction of structural CFS section and reinforced concrete deck slab. This reduces

the distance from the neutral-axis to the top of the deck and reduces the compressive bending stress in the CFS sections.

## **2. Previous Work**

The population growth in the world has an increase in the demand of residential construction and houses. Dannemann, (1982) [2] introduced low cost house structure system using cold formed steel sections, which is one of the most efficient and economic structural systems. In the past 25 years, wide growth of using cold formed steel sections in residential construction has been reported. Pekoz (1999) [3] states that, in the United States, there were about 500 houses built in light gauge steel in 1992. This number rose to 15,000 in 1993, 75,000 in 1994. In Australia, about 40000 new homes using load bearing cold formed steel framing are constructed per year (Hancock and Murray 1996 [4]). In Malaysia, recent development includes the increased application of light steel trusses consisting of cost-effective profiled cold-formed channels and steel portal frame systems as alternatives to the heavier traditional hot-rolled sections (CIDB, 2003) [5]. With fast and accurate manufacturing, ease handling and transportation, efficiency in cost and material, high strength-to-weight ratio, speed in erection, fully recyclable, durability, cold-formed steel sections could be an alternative economic structural components and frame systems for residential and commercial construction (Dannemann, 1982 [2]; Yu, 2000 [6]; Allen, 2006 [7]). The use of cold formed steel sections with concrete to shape composite beams can be a new alternative solution to replace hot rolled steel and reinforced concrete beams in small and medium size buildings (Hossain, 2005) [8]. Also, a significant reduction in the cost of light-gauge construction could be expected since the composite action will minimize the size of steel sections and thickness of concrete slabs needed. In the past 25 years, few researchers (Hanaor, 2000 [9]; Lawson et al., 2001 [10]; Hambro [11]; Lakkavali and Liu, 2006 [12]; Irwan, et al, 2009 [1]; Irwan, et al, 2011 [13] Wehbe, et al, 2011 [14]) had investigated the feasibility of designing cold formed steel section and concrete slab as composite beams. It was found that cold formed sections and concrete slabs could act compositely; cold formed steel section, the concrete slab and the degree of shear connection depends on the type, shape, spacing and configuration of the shear connector. In this research, a new technique of shear dowels for composite beams which consists of lipped channels cold formed steel beam and concrete slab has been used. The Innovative shear dowel (bent up half flange) is presented to connect the concrete slab and channel steel beam to make the composite action. The proposed shear dowel is easy to fabricate.

## **3. The Experimental Program**

Seven specimens were tested to study the behavior and capacity of the proposed composite beams. The test parameters include the shape of shear dowel, the concrete slab thickness and the CFS thickness. The specimens were tested by using a four-point load bending test.

### **3.1. Test Specimens**

The test specimen is 2 m long and the span between two supports is 1.8 m. The width of the concrete slab is 50 cm. The CFS is lipped channel (the flange 50 mm wide, web 160 mm height and 20 mm lip). The welded wire fabric reinforcement consists of 5 mm diameter bar with spacing of 100 mm x 100 mm. The use of wire mesh in the slab has shown higher flexural stiffness and capacity. To increase the efficiency of the shear connection, a bent-up half flange is suggested as shear dowel as shown in figure (1).

These beams comprise three groups; these groups have different slab thickness and shear dowel shape as shown in table (1) and figure (2). The first group includes b1, b2 and b3 which have steel thickness 2, 3 and 4 mm respectively, these specimens have the same floor thickness (60 mm) and shear dowel (bent up to half flange along beam as in figure 1a). The second group includes b4 and b5 which have steel thickness 3 and 4 mm respectively, these two specimens have the same floor thickness (80 mm) and shear dowel (bent up to half flange along beam). The third group includes b6 and b7 which have steel thickness 2 and 3 mm respectively, these two specimens have the same floor thickness (60 mm) and shear dowel (partial bent up to half flange every 40 cm as in figure 1b).

**Table (1):** Details of specimens for experimental work.

| group     | Specimen No. | Slab thickness (mm) | Steel thickness (mm) | Shape of steel section  | Figure |
|-----------|--------------|---------------------|----------------------|---|--------|
| <b>L1</b> | b1           | <b>60</b>           | <b>2</b>             |    | 1.3    |
|           | b2           |                     | <b>3</b>             |   |        |
|           | b3           |                     | <b>4</b>             |   |        |
| <b>L2</b> | b4           | <b>80</b>           | <b>3</b>             |   |        |
|           | b5           |                     | <b>4</b>             |   |        |
| <b>L3</b> | b6           | <b>60</b>           | <b>2</b>             |  |        |
|           | b7           |                     | <b>3</b>             |   |        |



**Figure (1a):** Bent-up half flange of channel along beam as shear dowel.

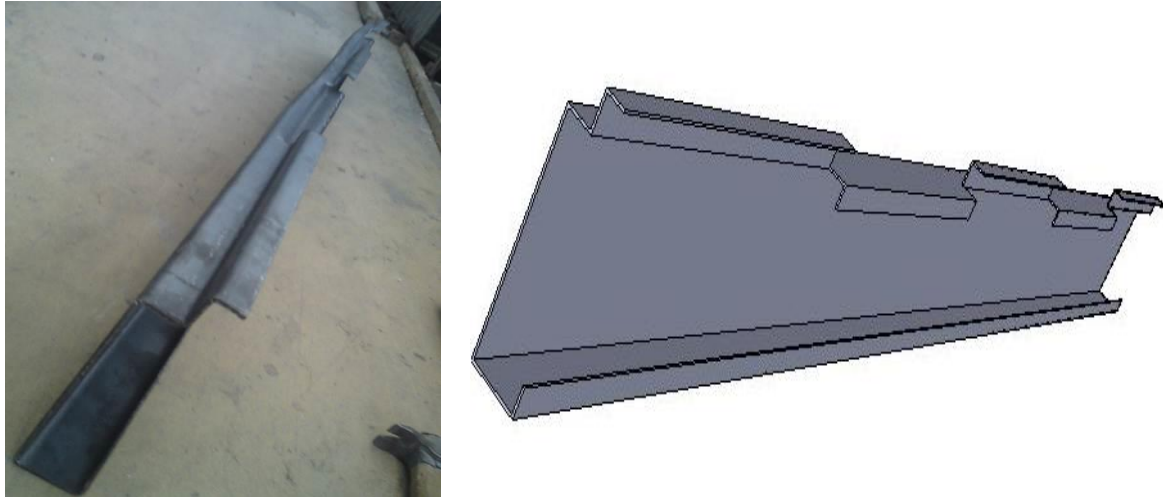


**Figure (1b):** Partial bent-up half flange of channel as shear dowel.

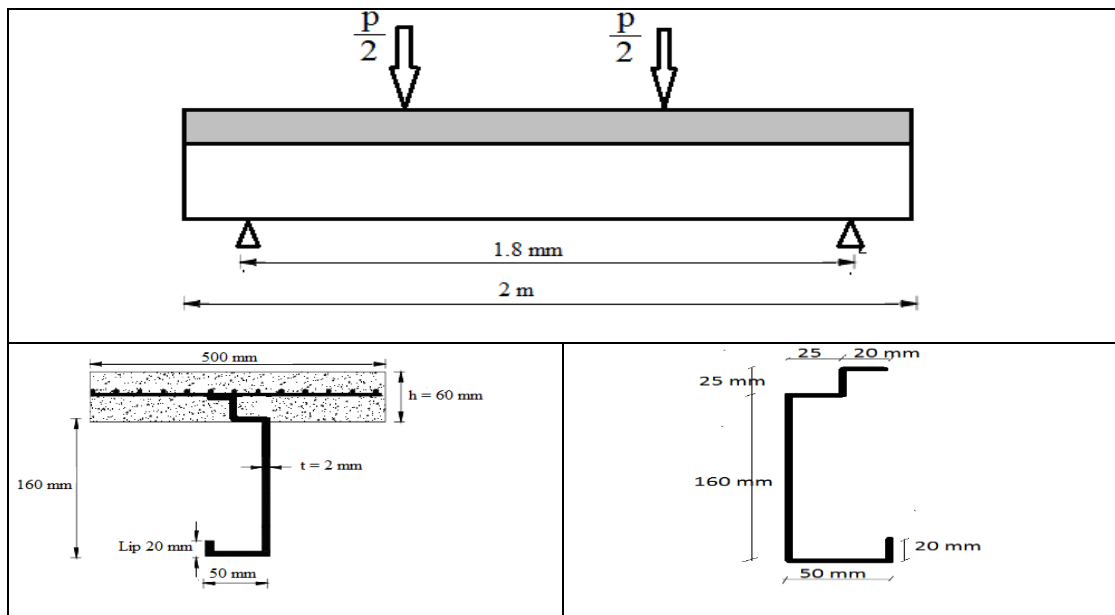


**Figure (2):** CFS–concrete composite beam specimen.

### 3.2. Test Setup and Procedure

All CFS–concrete composite beams specimens were tested using a Universal Testing Machine subjected to four point bending test system. Specimens were supported on a pin at one end and a roller at the other end to simulate a simple supported beam structure. The instrumentation setup is shown in Fig. (3). Deflections at the bottom flange of the steel section were monitored at the center and third-points using LVDT. A bubble level was used to level up the transducers in order to read the best possible vertical displacements (Deflection). The strain gauges were installed in the mid-span of the bottom flange and top web of CFS beam as well as at the bottom and top surface of the concrete slab. All measurements were connected to the data logger. To prevent local buckling, a steel plate of U shape was added at the two supports. The load applied to the beam was increased gradually and all measurements after each increment were

recorded. Thereafter, the beam was loaded in increments until failure of the specimen was observed or until a very large deflection occurred.

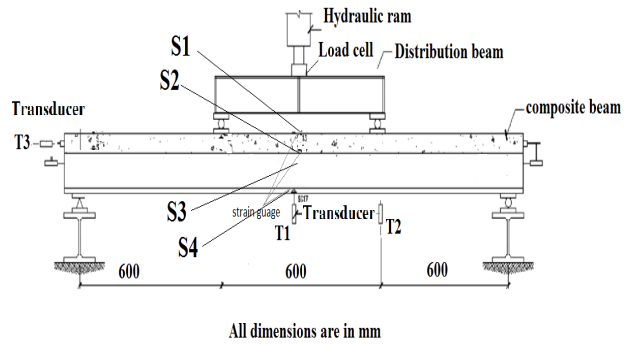


**Figure (3):** Large-scale test arrangement for composite beam.

### 3.3. Material Properties of Specimens

#### 3.3.1 Steel Bars and Steel Plates

Tension tests were performed on three steel bars specimens; also a tension test was carried out on steel plate and Strain gauge was used to determine the actual stain and Young's modulus in each type. Table (2) gives the mechanical properties of the reinforcing bars used and steel plate (CFS) types.

#### 3.3.2 Concrete

The gravel used in this work was local one having specific gravity and volume weight of 2.53 and 1.52 gm/cm<sup>3</sup>, respectively and maximum nominal size of 20 mm. Sand from natural sources having a specific gravity 2.63, volume weight and fineness modulus of 1.73 gm/cm<sup>3</sup>, 3.19, respectively, were used. Ordinary Portland cement was used in this study, the specific gravity 3.15, surface area 3200 cm<sup>2</sup>/gm, initial setting time 2.25hr and final setting time 4.25 hr. The concrete mix was designed to have a 28 days cubic strength of about 27 N/mm<sup>2</sup>. The concrete mix proportion is given in details in table (3). Longitudinal reinforcing steel and steel plate (CFS) was mild steel of grade 24/35.

**Table (2):** Mechanical properties of reinforcement steel.

| Nominal diameter mm | Actual dia. mm | Yield stress (N/mm <sup>2</sup> ) |                           | ultimate stress (N/mm <sup>2</sup> ) |              | Elongation% |
|---------------------|----------------|-----------------------------------|---------------------------|--------------------------------------|--------------|-------------|
|                     |                | test result                       | ESS <sup>#</sup> 203/2008 | test result                          | ESS 203/2008 | test result |
| 5                   | 4.8            | 265                               | 240                       | 406                                  | 350          | na          |
| Steel plate         | 2 <sup>*</sup> | 272                               | 240                       | 381                                  | 350          | 28 %        |

(\*) thickNess of steel plate (CFS)

(#)ESS: Egyption specifications

**Table (3):** the concrete mix proportion

| Cement kg/m <sup>3</sup> | Water L/m <sup>3</sup> | Sand kg/m <sup>3</sup> | Gravel kg/m <sup>3</sup> |
|--------------------------|------------------------|------------------------|--------------------------|
| 350                      | 175                    | 400                    | 800                      |

For each concrete batch, compressive strength, tensile strength and modulus of elasticity tests were performed on 15\*15\*15 cm cubes. The average compressive, tensile strength and modulus of elasticity were 27 N/mm<sup>2</sup>, 3.12 N/mm<sup>2</sup> and 23.3 KN/mm<sup>2</sup>, respectively.

#### 4. Analysis of Experimental Results

The purpose of the flexural bending test for full scale specimen was to study the behavior of CFS–concrete composite beams and to determine the efficiency of bent up part of flange of the channel as shear dowel. The results that were sustained by testing of each specimen are summarized in Table (4).

**Table (4):** Experimental results of ultimate loads for specimens.

| group | Specimen No. | t <sub>f</sub><br>m | t <sub>steel</sub><br>(m<br>m) | Ultimate load, P <sub>u</sub> (kN) | Deflection at P <sub>u</sub> , δ <sub>u</sub> (mm) | Ultimate moment, M <sub>u,exp</sub> (kN.m) | Failure mode      |
|-------|--------------|---------------------|--------------------------------|------------------------------------|--|--|-------------------|
| L1    | b1           | 60                  | 2                              | 46.1                               | 19.90  | 13.83                                      | Buckling of CFS   |
|       | b2           |                     | 3                              | 73.5                               | 20.10  | 22.05                                      | Concrete crushing |
|       | b3           |                     | 4                              | 94.7                               | 15.76  | 28.41                                      |                   |
| L2    | b4           | 80                  | 3                              | 77.3                               | 16.66  | 23.19                                      | Concrete crushing |
|       | b5           |                     | 4                              | 130.6                              | 16.39  | 39.18                                      |                   |
| L3    | b6           | 60                  | 2                              | 47.3                               | 23.65  | 14.19                                      | Buckling of CFS   |
|       | b7           |                     | 3                              | 81.6                               | 17.79  | 24.48                                      | Concrete crushing |

#### 4.1. Parametric Study

##### 4.1.1 Shear Dowel Enhancements

Testing of specimens in Groups L1 and L3 was carried out to investigate the effect of different types of proposed shear dowel enhancement in CFS–concrete composite beams. The ultimate loads sustained by all specimens are summarized in Table (4). It was found that a CFS–concrete composite beam specimen with suggested shear dowel enhancements showed an increase in capacity of ultimate moment. The ultimate capacity of Specimen (b6) (bent up half flange each 40 cm) is 2.6% higher than that of Specimen (b1) (full bent up half flange). The ultimate capacity of Specimen (b7) (partially bent up half flange) shows an increase of 11% in the ultimate capacity over Specimen (b2) (full bent up half flange). Therefore, it can be concluded that the ultimate moment resistance of the CFS–concrete composite beam with partial bent up half flange each 40 cm is better than the CFS–concrete composite beam with bent up half flange along beam (full bent up of half flange as shear dowel).

##### 4.1.2 Thickness of CFS

Specimens in Group L1, L2 and L3 were tested in order to investigate the effect of different thicknesses of CFS. Table (4) and figure (4) show the ultimate moment obtained experimentally using 2 mm, 3 mm and 4mm thick CFS with full and partial bent up half flange enhancement. In the first group; specimen (b3), 4 mm thick, has an ultimate moment of 28.41 kN.m while specimen (b2), 3 mm thick, has an ultimate moment of 22.05 kN.m. Specimen (b1), 2 mm thick, has an ultimate moment of 13.83 kN.m. These results lead to an increase of 59.44% between b1 and b2, while the increase between b2 and b3 was 28.84%. In the second group; specimen (b5), 4 mm

thick, has an ultimate moment of 39.18 kN.m while the specimen (b4), 3 mm thick, has an ultimate moment of 23.19 kN.m. These results lead to an increase of 68.95% between b4 and b5. In the third group; specimen (b7), 3 mm thick, has an ultimate moment of 24.48 kN.m while the specimen (b6), 2 mm thick, has an ultimate moment of 14.19 kN.m. These results lead to an increase of 72.52% between b4 and b5.

### 4.1.3 Thickness of Concrete Slab

Specimens in Group L1 and L2 were tested to investigate the effect of different thicknesses of concrete slab as shown in table (4). Specimen (b4), slab thickness was 80 mm, has an ultimate moment of 23.19 kN.m while the specimen (b2), slab thickness was 60 mm, has an ultimate moment of 22.05 kN.m. These results lead to an increase of 5.17% between b2 and b4. Specimen (b5), slab thickness was 80 mm, has an ultimate moment of 39.18 kN.m while the specimen (b3), slab thickness was 60 mm, has an ultimate moment of 28.41 kN.m. These results lead to an increase of 37.91% between b4 and b5. This is expected, since the higher thickness of slab increases the capacity of the member because of the increase of the compression zone. Generally, increasing the concrete slab thickness for a constant grade of concrete and steel and the thickness of steel for all beams is accompanied by an increase in the ultimate load values.

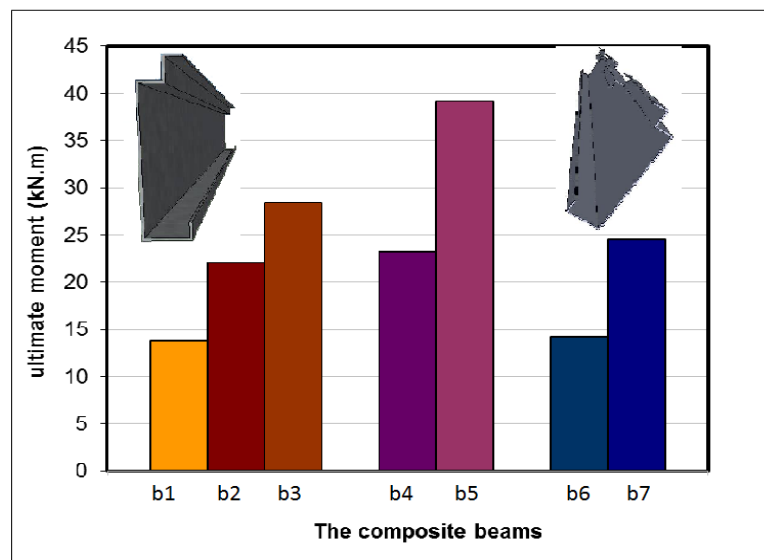


**Figure (4):** The ultimate moment for the experimental results.

### 4.2 Load-Deflection Behavior and Failure Mechanisms

Figures (5) to (7) show the typical load versus mid-span deflection curves and load versus deflection under the load for large-scale CFS–concrete composite beam specimens. Figures from (8) to (10) show the load versus relative horizontal displacement (slip) curves. The figures indicate that slip at ultimate load in specimen's b6 and b7 is less than the other specimens. In general, the cracking patterns of all specimens do not vary much from one another. All specimens developed primary cracks below the loading positions until failure. The failure modes observed can be classified into two types, concrete crushing or buckling of CFS at support. The modes of failure of all specimens are summarized in Table (4). As shown in Table (4), specimens having 3 mm and 4 mm thick CFS exhibited a concrete crushing failure mode, while specimens

having 2 mm thick CFS exhibited buckling of web of CFS at support. Figures (11) to (15) show the typical cracking patterns and failure modes of all the specimens.

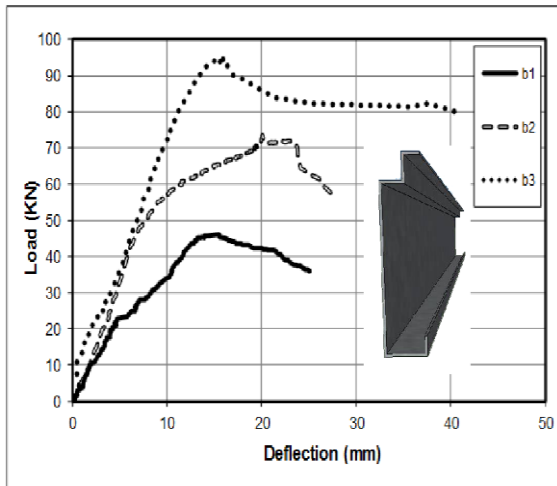


**Figure (5):** Load - deflection curve at mid span of tested group L1

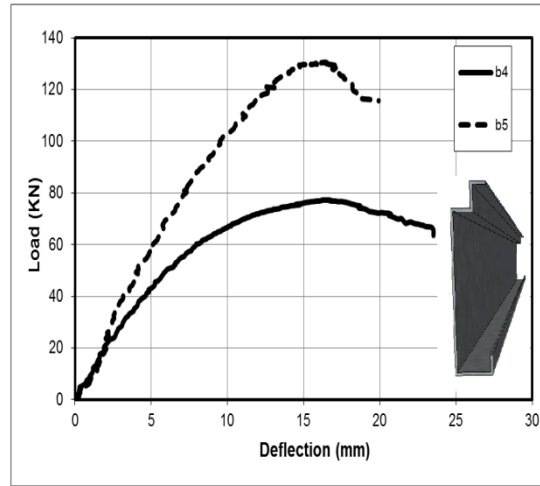


**Figure (6):** Load - deflection curve at mid span of tested group L2

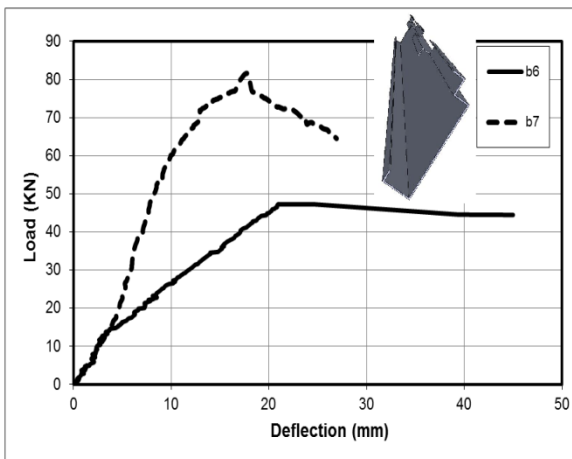


**Figure (7):** Load - deflection curve at mid span of tested group L3

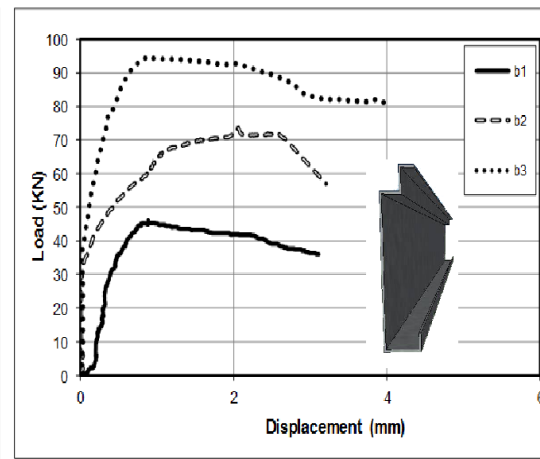


**Figure (8):** Load – horizontal displacement (slip) of tested group L1

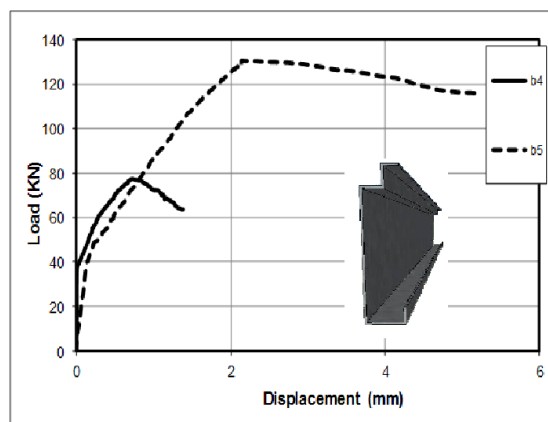


**Figure (9):** Load – horizontal displacement of tested group L2

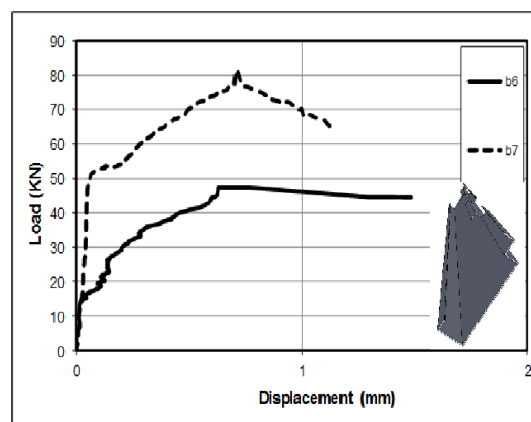


**Figure (10):** Load – horizontal displacement of tested group L3



**Figure (11):** Typical large-scale test specimen (b1) failed due to buckling of CFS at support.



**Figure (12):** Typical large-scale test specimen (b2) failed due to concrete crushing.



**Figure (13):** Typical large-scale test specimens (b3),(b4) and (b5) failed due to concrete crushing.



**Figure (14):** Typical large-scale test specimen (b6) failed due to buckling of CFS at support.



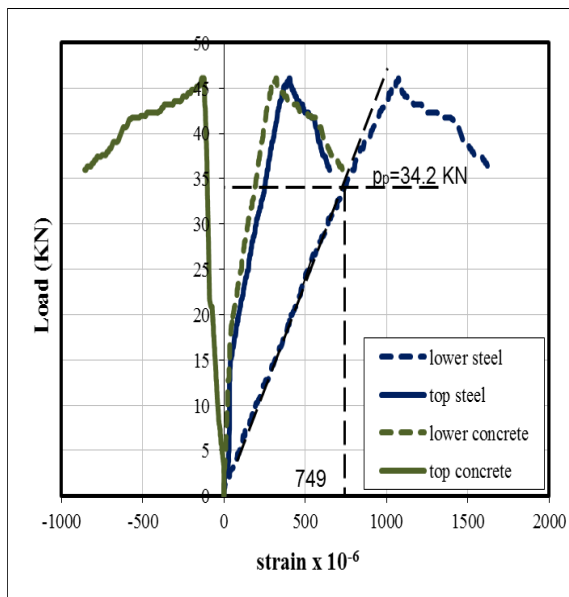
**Figure (15):** Typical large-scale test specimen (b7) failed due to concrete crushing.

### 4.3 Load- Strain Relationships

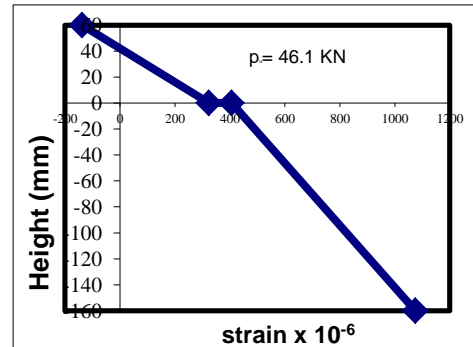
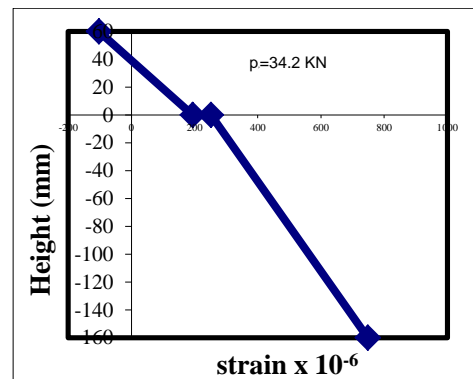
The measurement of strain on concrete slab and steel beam at the middle of the tested beams was plotted against the applied load. The relationship between the applied loads versus strain at the middle of tested beam is shown in figures (16 to 22). It is obvious from the shown curves that the common strain curve fluctuates for both concrete and steel strains in specimens, from positive to negative values, and this can be attributed to different composite action behavior, where the bottom surface strain (steel strain) remained tension throughout the loading cycle for most of the specimens.

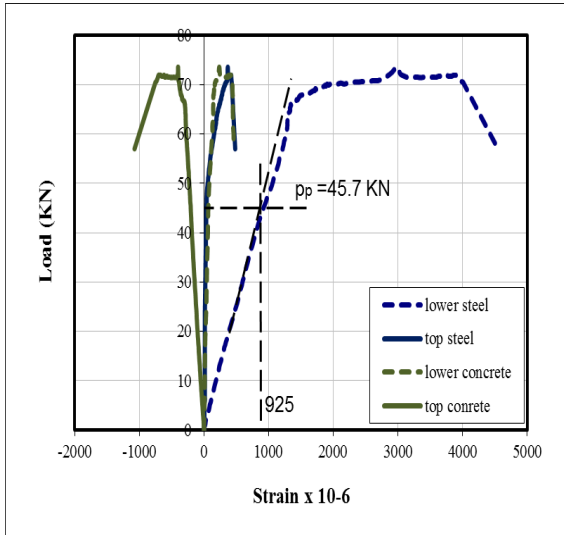
### 4.4 Neutral Axis and Assessment of Composite Action

The integrity of the composite actions was assessed by measuring the strain distributions of a section under applied bending loads. The strain gauges were installed at mid-span section at the bottom flange, at top web of proposed CFS, and at top and bottom of the concrete slab, respectively. The strain values versus the location of strain gauges were plotted for proportional limit and ultimate loads for each specimen. They are shown in figures 18 to 24. The neutral axis of section moves during loading phase, due to the loss of specimen stiffness caused by concrete cracking, longitudinal end slip, or buckling of CFS. The figures indicate that the top surface of concrete slab is subjected to compressive strain, while the bottom surface of concrete slab is subjected to tensile strain. CFS is subjected to tensile strain along its height.

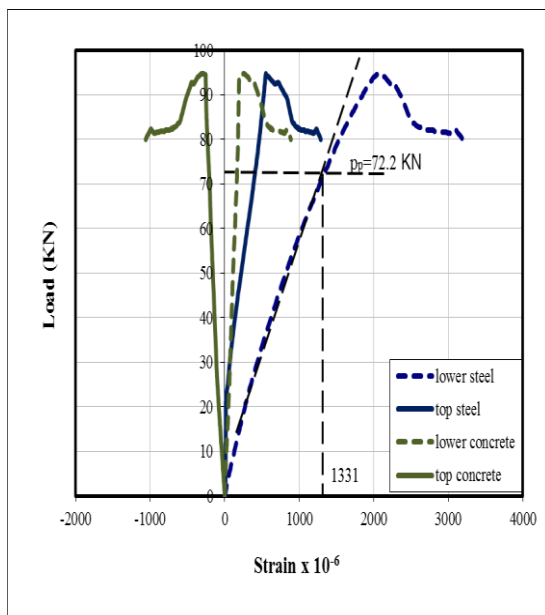
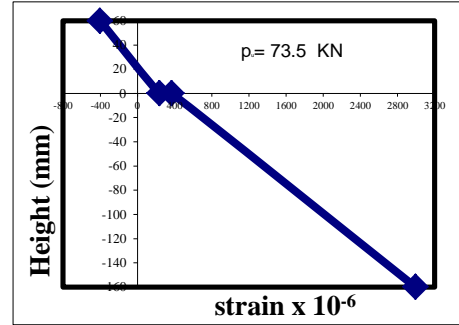
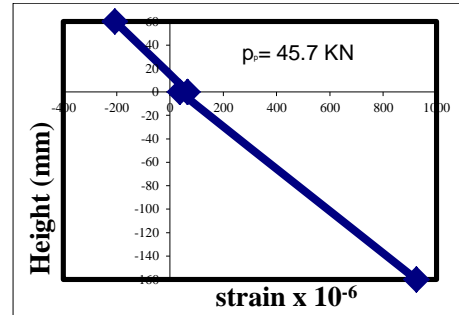


**Figure (16):** Load – longitudinal strain curve of tested specimen No 1  
(P p): proportional limit.

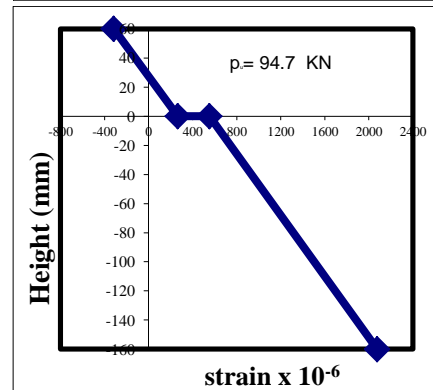
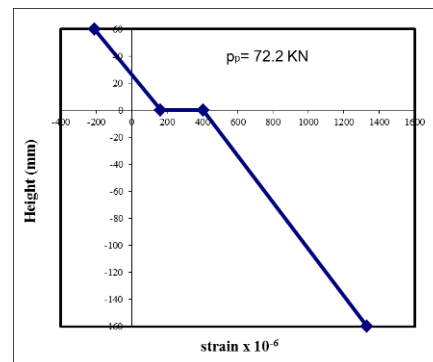


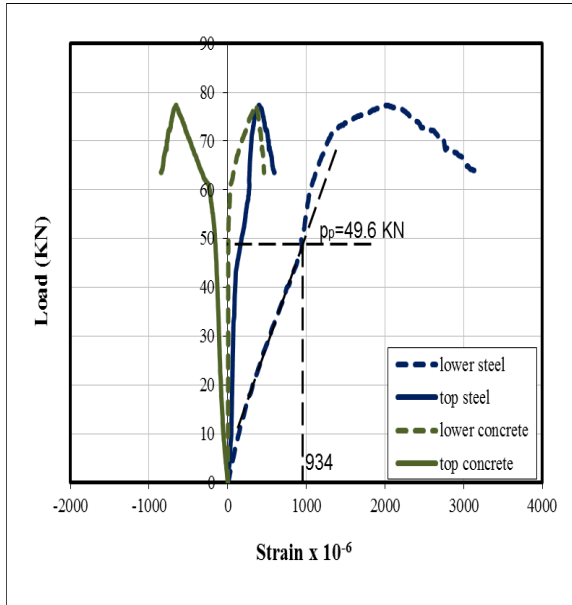


**Figure (17):** Load – longitudinal strain curve of tested specimen No 2

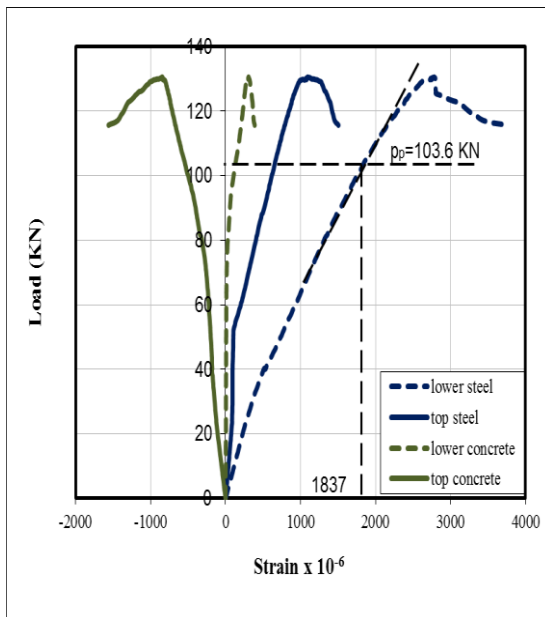
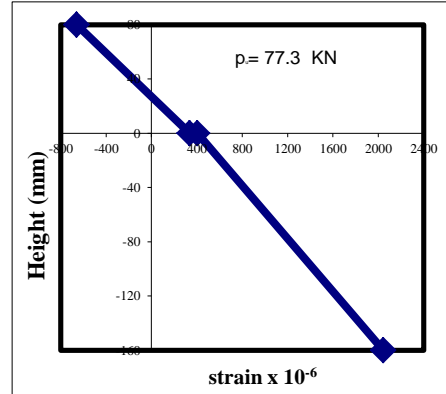
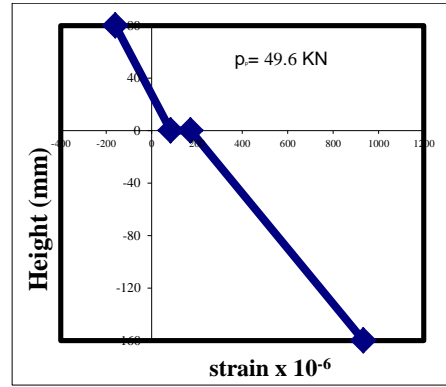


**Figure (18):** Load – longitudinal strain curve of tested specimen No 3

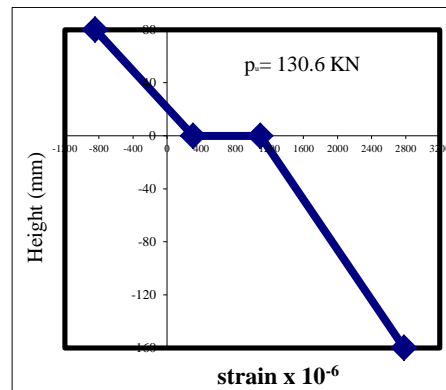
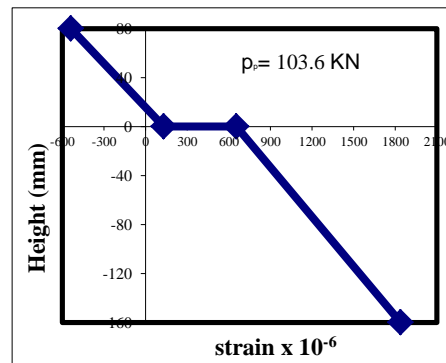


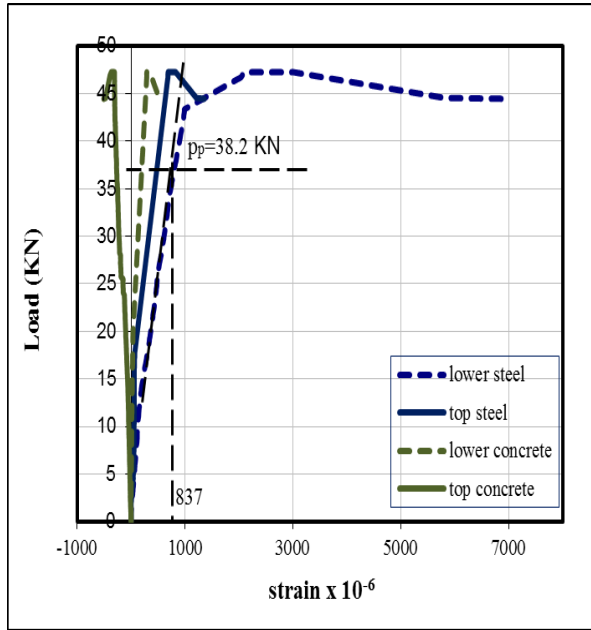


**Figure (19):** Load – longitudinal strain curve of tested specimen No 4

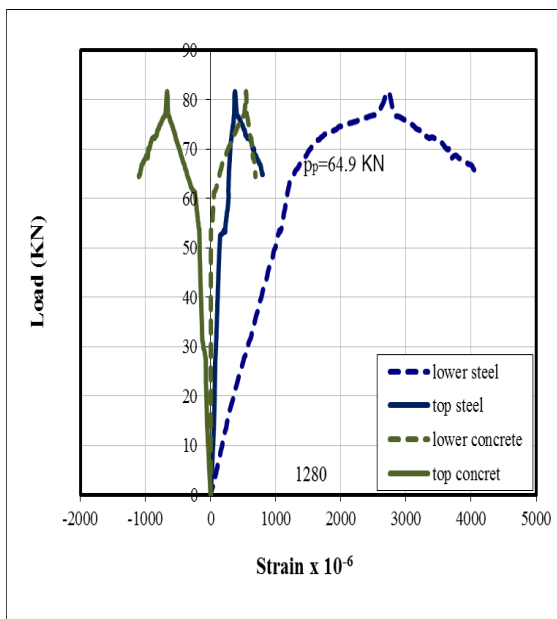
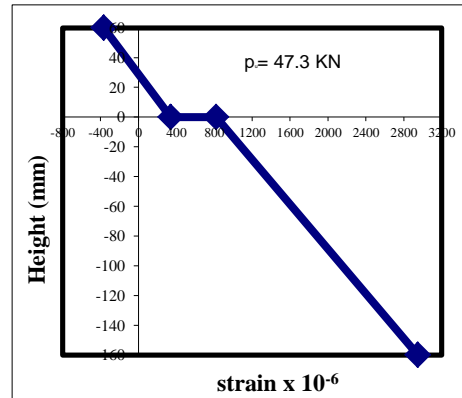
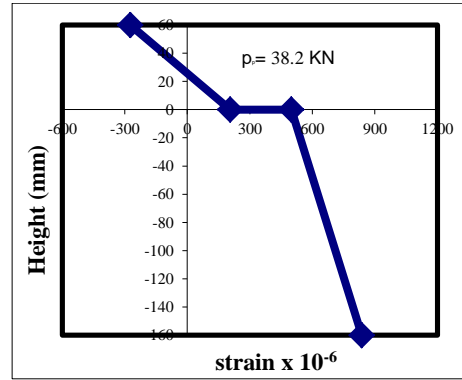


**Figure (20):** Load – longitudinal strain curve of tested specimen No 5

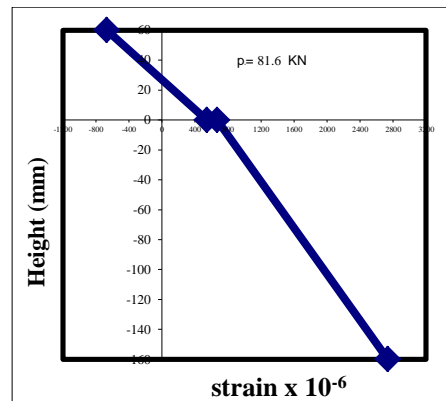
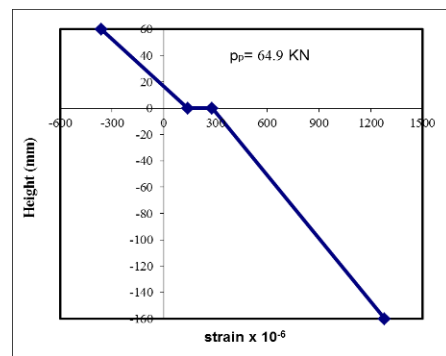




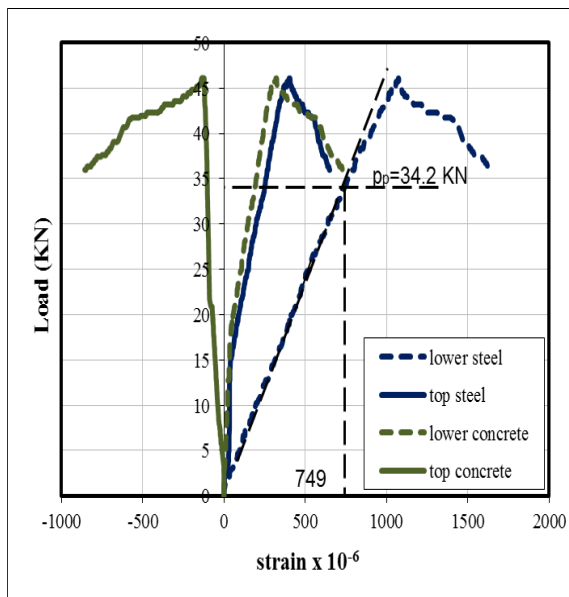
**Figure (21):** Load – longitudinal strain curve of tested specimen No 6



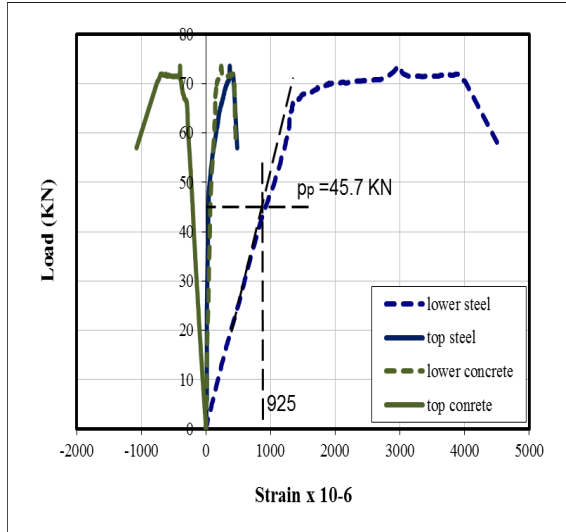
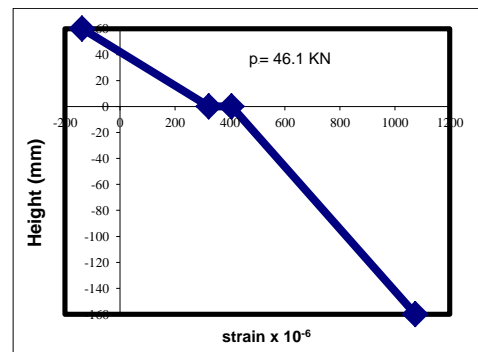
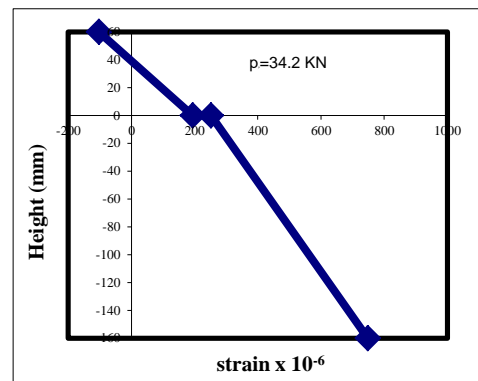
**Figure (22):** Load – longitudinal strain curve of tested specimen No 7



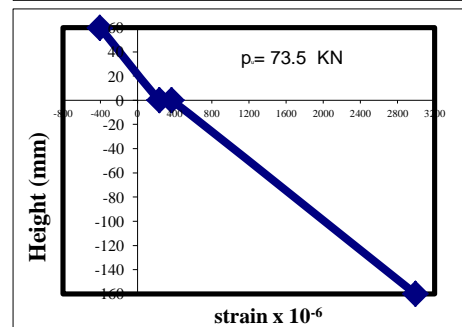
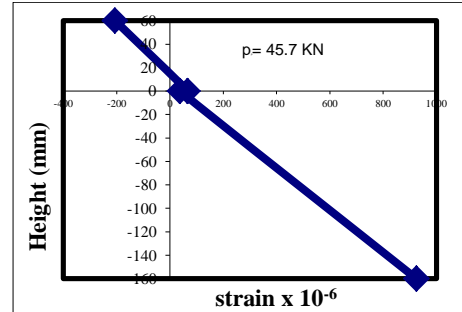
## 5. Evaluation of Test Results

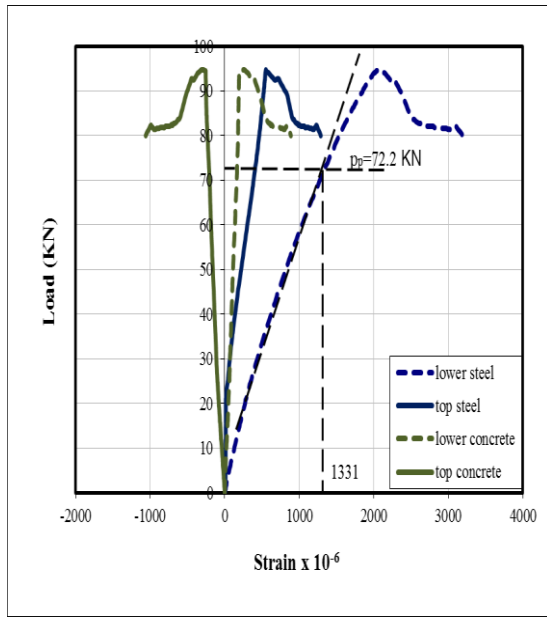


**Figure (16):** Load – longitudinal strain curve of tested specimen No 1  
(P p): proportional limit.

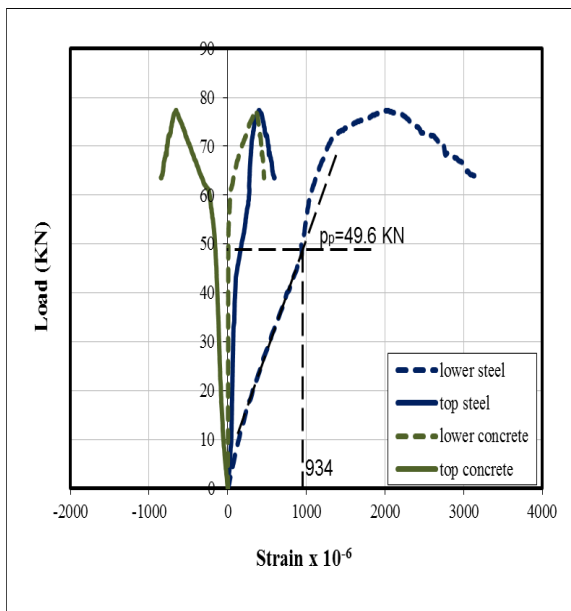
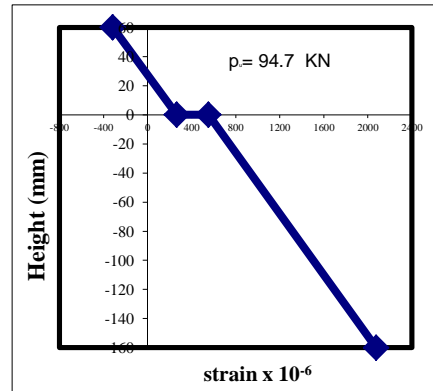
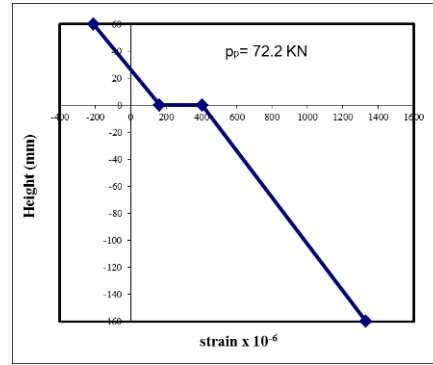


**Figure (17):** Load – longitudinal strain curve of tested specimen No 2

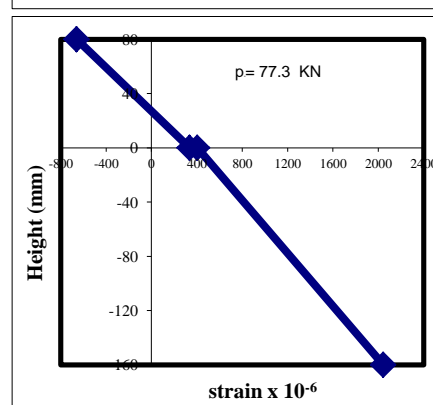
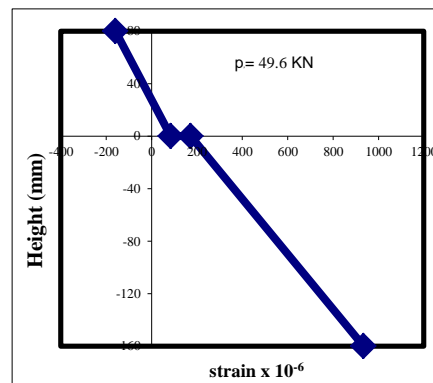


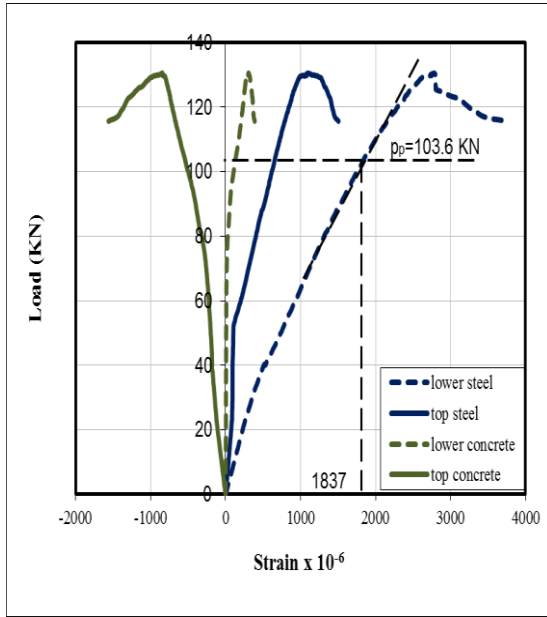


**Figure (18):** Load – longitudinal strain curve of tested specimen No 3

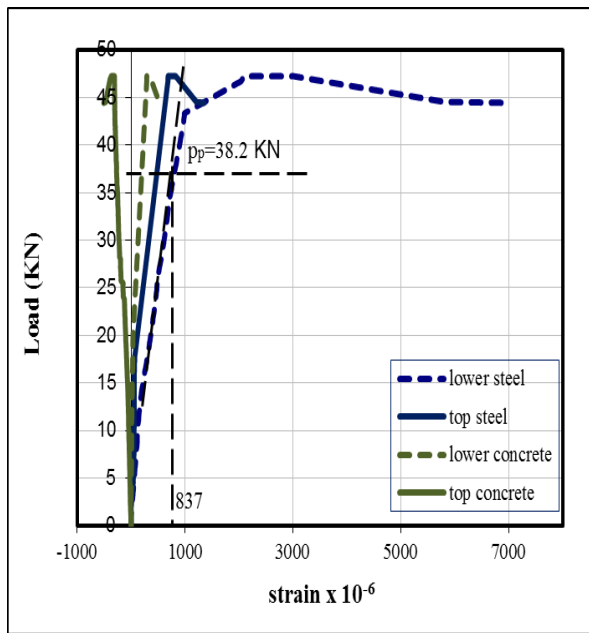
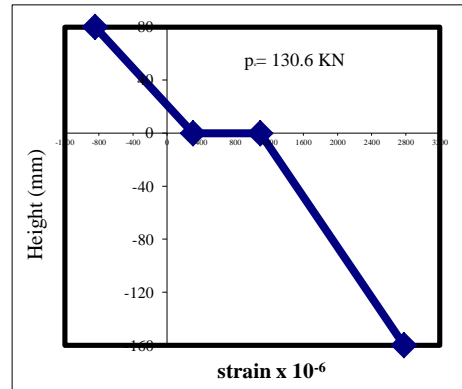
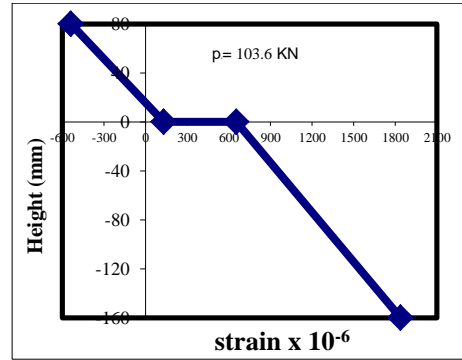


**Figure (19):** Load – longitudinal strain curve of tested specimen No 4

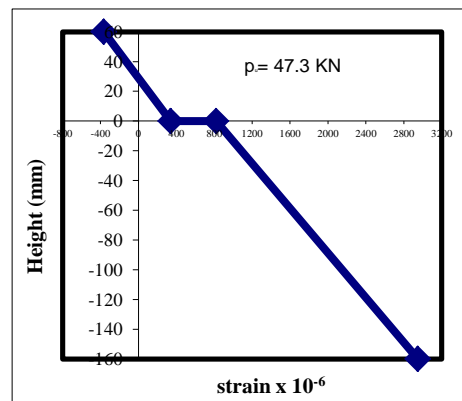
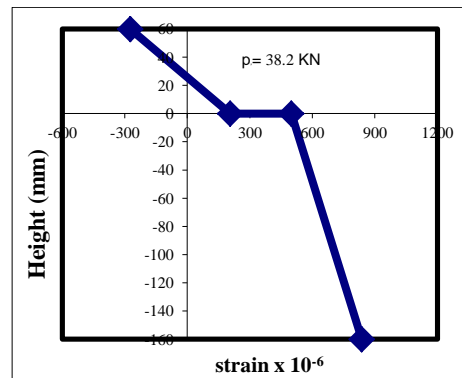




**Figure (20):** Load – longitudinal strain curve of tested specimen No 5



**Figure (21):** Load – longitudinal strain curve of tested specimen No 6



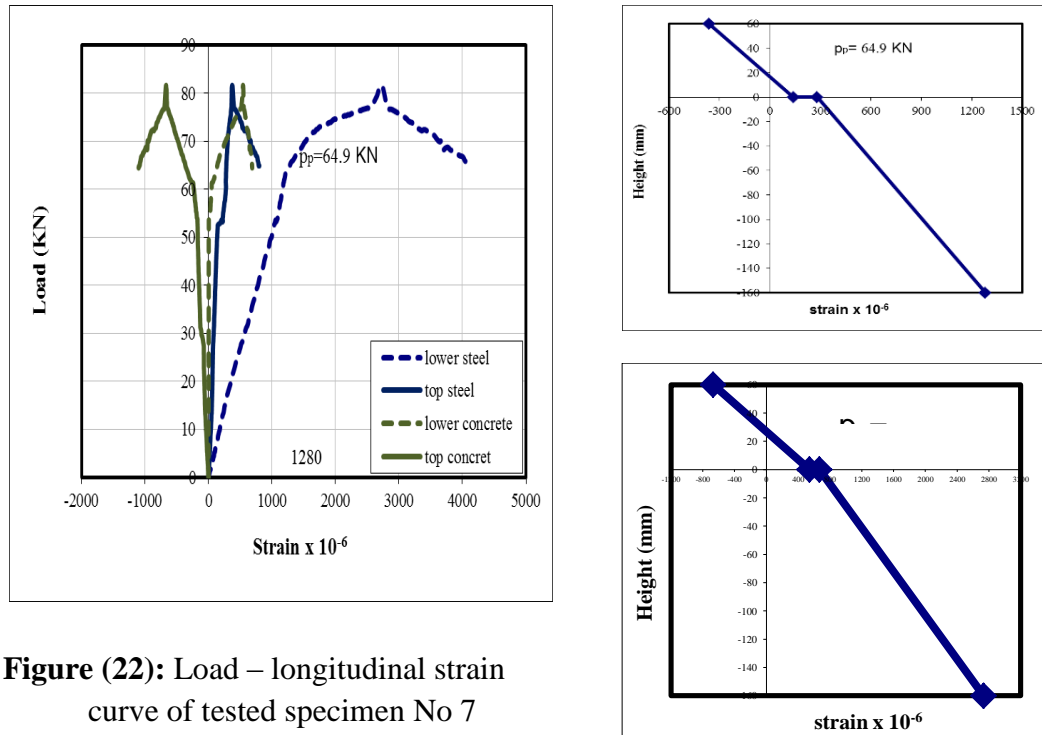


**Figure (22):** Load – longitudinal strain curve of tested specimen No 7

## 5. Evaluation of Test Results

The resulting theoretical ultimate moment capacities are compared to those from experiments as shown in Table (5). The resistance of studied sections is determined using plastic analysis principles. It is assumed that the strains across the section are sufficiently high that the CFS stresses are at their yield values throughout the section and that the concrete has reached its compressive strength. Plastic stress blocks are rectangular, unlike elastic stress blocks which are triangular. Because the slab section is reinforced with a layer of reinforcement, it shows a very ductile behavior and can be assumed to behave as a perfectly plastic material with different properties in compression and tension. Manual calculations using the principle analysis depicted that the ultimate strength capacity of CFS composite beams can be efficiently estimated by using conventional equilibrium procedures and the constitutive laws prescribed by EC4 [15] using standard tests for the materials. Table (5) shows the comparison between analytical and experimental results. The ratios of experimental to predicted ultimate moments varied from 0.8 to 1.04.

**Table (5):** Comparison of experimental and theoretical analysis

| Group | Specimens | Experimental results                | Calculated/Theory analysis           | Strength ratio |
|-------|-----------|-------------------------------------|--------------------------------------|----------------|
|       |           | Ultimate Moment, $M_{u,exp}$ (kN.m) | Ultimate Moment, $M_{u,theo}$ (kN.m) |                |
| L1    | b1        | 13.83                               | 17.4                                 | 0.80           |
|       | b2        | 22.05                               | 25.62                                | 0.86           |
|       | b3        | 28.41                               | 33.6                                 | 0.85           |
| L2    | b4        | 23.19                               | 28.8                                 | 0.81           |
|       | b5        | 39.18                               | 37.8                                 | 1.04           |
| L3    | b6        | 14.19                               | 17.4                                 | 0.82           |
|       | b7        | 24.48                               | 25.62                                | 0.96           |

## 6. Conclusions

Based on the results of large-scale slab specimens, the following can be concluded:

- 1- In general, the cracking patterns of all specimens do not vary from one another and all specimens developed primary cracks below the loading positions until failure.
- 2- CFS specimens with thickness of 3 mm and 4 mm exhibited concrete crushing failure mode, while CFS specimens with thickness of 2 mm exhibited buckling of CFS failure mode at supports.
- 3- CFS–concrete composite beam specimens with proposed shear dowel enhancements showed an increase in capacity of ultimate moment.
- 4- Specimen with partial bent up of half flange every 40 cm shows an increase of 11% in the ultimate capacity over Specimen with bent up of half flange along beam.
- 5- Increasing thickness of CFS for constant grades of concrete and steel and same thickness of slab for all composite beams is accompanied by an increase in the ultimate moment values by 28% to 73%.
- 6- Increasing of concrete slab for constant grades of concrete and steel and same thickness of CFS for all beams is accompanied by an increase in the ultimate load values by 5% to 38%.

## REFERENCES

- [1] Irwan, M., Hanizah, A. and Azmi, I. (2009). Test of shear transfer enhancement in symmetric cold-formed steel concrete composite beams. *Journal of Constructional Steel Research*, 65(12), 2087-2098.
- [2] Dannemann, R. W. (1982). Cold Formed Standard Steel Products in a Low Cost House Construction Method. Sixth international specialty conference on cold-formed steel structures. St. Louis, Missouri, USA, 653-674.
- [3] Pekoz, T. (1999). Possible Future Developments in the Design and Application of Cold-Formed Steel. Fourth international conference. Light-Weight Steel and Aluminium Structures. Espoo, Finland.
- [4] Hancock, G. J. and Murray. T. M. (1996). Residential Applications of Cold Formed Structural Members In Australia. Thirteenth International Specialty Conference on Cold-Formed Steel Structures. St. Louis, Missouri, USA, 505-511.
- [5] CIDB, (2003). Survey on the usage of Industrialised Building Systems (IBS) in Malaysian Construction Industry. CIDB Malaysia publication.
- [6] Yu, W. W. (2000). Cold-Formed Steel Design. (3rd ed.) New York, John Wiley & Sons, Inc.
- [7] Allen, D. (2006). Mid-Rise Construction Detailing issues with Cold-Formed Steel and Compatible Construction Materials. ASCE, Structures.
- [8] Hossain, A. (2005). Designing thin-walled composite-filled beams. *Proceedings of the Institution of Civil Engineers, Structures & Buildings*, 158(SB4), 267-278.
- [9] Hanaor, A. (2000). Tests of composite beams with cold-formed sections. *Journal of Constructional Steel Research*, 54(2), 245–264.
- [10] Lawson, R. M., Popo-Ola, S. O. and Varley, D. N. (2001). Innovative development of light steel composites in buildings. In: Eligehausen, R. (ed.) *International Symposium*

on Connections between Steel and Concrete. Stuttgart, Germany RILEM Publications SARL.

[11] Hambro® Composite Floor Joist Systems (2004). Handbook of Hambro® D500. Hambro®, available from <http://www.hambrosystems.com/>.

[12] B. S. Lakkavalli and Y. Liu, 2006. Experimental Study of Composite Cold-formed Steel C section Floor Joists. *Journal of Constructional Steel Research*. 62: 995–1006.

[13] J. M. Irwan, A. H. Hanizah, I. Azmi, and H. B. Koh. 2011. Large-scale Test of Symmetric Cold-formed Steel (CFS)–concrete Composite Beams with BTTST Enhancement. *Journal of Constructional Steel Research*. 67: 720–726.

[14] Wehbe, N., Wehbe, A., Dayton, L. and Sigl, A. (2011). Development of Concrete/Cold Formed Steel Composite Flexural Members. *Structures Congress*, ASCE, 3099-3109.

[15] European Committee for Standardization. (2004). EN1994-1-1. Brussels: European Committee for Standardization.